Nature of the interaction of heparin with acidic fibroblast growth factor. Biochemistry 32:5480-5489

ARTICLE *in* BIOCHEMISTRY · MAY 1993

Impact Factor: 3.02 · DOI: 10.1021/bi00071a026 · Source: PubMed

Reprinted from Biochemistry, 1993, 32.

Nature of the Interaction of Heparin with Acidic Fibroblast Growth Factor†

Henryk Mach,* David B. Volkin, Carl J. Burke, and C. Russell Middaugh

Department of Pharmaceutical Research, Merck Research Laboratories, WP26-331, West Point, Pennsylvania 19486

Robert J. Linhardt,* Jonathan R. Fromm, and Duraikkannu Loganathan

Division of Medicinal and Natural Products Chemistry, College of Pharmacy, University of Iowa, Iowa City, Iowa 52242

Lars Mattsson

Pharmacia Biosensor, 800 Centennial Avenue, Piscataway, New Jersey 08854

Received June 12, 1992; Revised Manuscript Received February 9, 1993

ABSTRACT: The binding of human acidic fibroblast growth factor (aFGF) to heparin has been analyzed by a variety of different approaches to better elucidate the nature of this protein/sulfated polysaccharide interaction. Static and dynamic light scattering as well as analytical ultracentrifugation analyses indicates that 14–15 molecules of aFGF can bind to a 16-kDa heparin chain, with approximately 10 of these bound relatively uniformly to high-affinity sites. The dissociation constants of these latter sites are estimated to be approximately 50–140 nM on the basis of surface plasmon resonance experiments in which the association and dissociation rates of aFGF interaction with immobilized heparin were measured. The size of the binding site of aFGF on heparin was also determined by heparin lyase digestion of aFGF/heparin complexes followed by isolation and characterization of protected oligosaccharides. The smallest aFGF-protected oligosaccharide comigrated with ΔUA2S(1→4)-α-D-GlcNp2S6S(1→4)-α-L-IdoAp-2S(1→4)-α-D-GlcNp2S6S (where ΔUA represents 4-deoxy-α-L-*threo*-hex-4-enopyranosyluronic acid and S is sulfate). Thus, aFGF appears to bind at high density (one molecule every 4–5 polysaccharide units) and with high affinity to heparin. This potentially provides a concentrated, stabilized storage form of the growth factor that can be released for receptor-mediated cellular activation in response to the proper stimuli. It is also possible that close proximity of aFGF molecules on the highly sulfated regions of heparan chains may be involved in the induction of receptor aggregation as suggested by Ornitz et al. [Ornitz, D. M., Yayon, A., Flanagan, J. G., Svahn, C. M., Levi, E., & Leder, P. (1992) *Mol. Cell. Biol. 12*, 240–247].

A surprisingly large number of proteins bind to polyanionic substances such as heparin (Jackson et al., 1991). One class of proteins that manifests a particularly high affinity for sulfated polysaccharides is the mitogenic heparin-binding growth factors, the prototypic examples of which are acidic and basic fibroblast growth factor (aFGF[1] and bFGF) [reviewed by Burgess and Maciag (1989)]. Their interaction with polyanionic glycosaminoglycans is thought to be of functional significance with these extracellular matrix molecules serving as storage depots for the growth factors and protecting them from various degradative processes (Vlodavsky et al., 1991).

Some general features of the polyanion binding site of the FGFs are now known. The minimal size of sulfated polysaccharide necessary to stabilize aFGF from thermal unfolding consists of four monosaccharide units (Volkin et al., 1992, 1993) with less direct measurements (Uhlrich et al., 1986; Barzu et al., 1989; Sudhalter et al., 1989) suggesting a similar structural requirement. Despite this observation, a surprisingly wide diversity of anionic species has been found to bind and physically stabilize aFGF in vitro. This includes substances as diverse as polyanionic polynucleotides, polypeptides and polysaccharides, small sulfated and phosphorylated compounds (e.g., inositol hexasulfate and tetrapolyphosphate), as well as moderate concentrations of sulfate ion itself (Dabora et al., 1991; Volkin et al., 1992, 1993). The only common feature among these agents appears to be their high density of negative charge. Thus, the interaction of aFGF with polyanions in vitro appears to be relatively nonspecific when compared to the better characterized stereochemical requirements of the heparin activation of thrombin/antithrombin III complex formation (Petitou et al., 1991).

A variety of evidence suggests the involvement of a cluster of basic residues (Lys112, Lys118, and Arg122 in human aFGF) in the polyanion binding site of the FGFs (Zhu et al., 1991; Eriksson et al., 1991; Zhang et al., 1991). Little is known about the stoichiometry of interaction of the FGFs with polyanions such as heparin. Indirect evidence suggests that multiple FGF molecules are probably capable of binding to a single sulfated polysaccharide chain (Sommer & Rifkin, 1989; Copeland et al., 1991), although this claim has been disputed (Lee & Lander, 1991). Dissociation constants of basic and acidic FGF with heparin have been estimated to be in the range of 2–3 and 60–90 nM, respectively (Moscatelli, 1987; Walicke et al., 1989; Lee & Lander, 1991). It has also recently been reported that heparin and heparin fragments containing six monosaccharide units and above promote the formation of bFGF dimers and trimers (Ornitz et al., 1992). In this work, we employ a variety of physical and biochemical

† Portions of this work were supported by NIH Grant GM38060 to R.J.L.
* To whom correspondence should be addressed.
[1] Abbreviations: aFGF, acidic fibroblast growth factor; bFGF, basic fibroblast growth factor; EDTA, ethylenediaminetetraacetic acid; PBS, phosphate-buffered saline; RU, resonance units; SDS, sodium dodecyl sulfate; PAGE, polyacrylamide gel electrophoresis; EDC, *N*-ethyl-*N*'-((diethylamino)propyl)carbodiimide; NHS, *N*-hydroxysuccinimide.

0006-2960/93/0432-5480$04.00/0

methods to directly probe the stoichiometry of the interaction of aFGF with heparin, estimate the corresponding dissociation constants, and characterize the chemical nature of the most stable heparin interaction site.

MATERIALS AND METHODS

Materials

Porcine intestinal mucosal and bovine lung heparin (16 kDa) were purchased from Hepar, and low molecular weight heparin (4.8 kDa) was from Calbiochem. Inositol hexasulfate and other polyanionic compounds were purchased from Sigma. A buffer (PBS) consisting of 6 mM sodium phosphate, 120 mM sodium chloride, 1 mM sodium sulfate, and 1 mM ethylenediaminetetraacetic acid (EDTA), pH 7.2, was employed in most studies unless otherwise indicated. Surfactant P20 (Tween 20) and an amine coupling kit containing *N*-hydroxysuccinimide (NHS), *N*-ethyl-*N'*-((diethylamino)propyl)carbodiimide (EDC), and 1 M ethanolamine hydrochloride, pH 8.5, were all obtained from Pharmacia Biosensor. The aFGF employed was prepared from transformed *Escherichia coli* as previously described (Thomas et al., 1984; Linemeyer et al., 1987). CNBr-activated Sepharose 4B (with a protein binding capacity of approximately 8 mg/mL) and heparin–agarose (0.75–0.80 mg of heparin/mL of bed) were purchased from Sigma. Heparin lyase I (EC 4.2.2.7) having a specific activity of 150 units/mg (1 unit = 1 μmol of product formed/min) was purified to apparent homogeneity from *Flavobacterium heparinum* as previously reported (Lohse & Linhardt, 1992). Heparin lyase II (no EC number) was prepared from the same organism and purified to apparent homogeneity. This enzyme had a specific activity of 15 units/mg (Lohse & Linhardt, 1992). Similar results could be obtained using commercially available enzymes of lower purity (Linhardt et al., 1990).

Light Scattering

Light scattering experiments at a 90° scattering angle were performed with a Malvern 4700 spectrometer (Malvern, England) equipped with a 5-W argon laser (Spectra Physics) (Middaugh et al., 1992). Quartz cuvettes (0.5 mL) were employed permitting aFGF concentration (~1 mg/mL) to be directly monitored by UV spectrophotometry during titrations. Hydrodynamic radii were calculated from a cumulant analysis of the autocorrelation function (Koppel, 1972). The scattering intensities from heparin itself were generally negligible, since the squared dn/dc ratio of aFGF/heparin was approximately 0.4 and at least a 10:1 excess of aFGF was employed for the stoichiometric analysis. Refractive index increments were determined with an Optilab 903 differential refractometer (Wyatt Technologies) calibrated with aqueous sodium chloride solutions.

Determination of the Average Number of aFGF Molecules Bound to Heparin

The total intensity of scattered light (I) is a weight average of the contributions from each of the species with scattering I_i and concentration c_i (Tanford, 1961):

$$I = \sum c_i I_i / \sum c_i \qquad (1)$$

If $\bar{n}$ is the average number of aFGF molecules bound to heparin (i.e., a heparin polymer partially saturated with a monomeric protein), the amount of aFGF bound to heparin will be given by $\bar{n}rC_P$, where r is the ratio of protein to polymer molecular weight and C_P is the concentration (in milligrams per milliliter) of the heparin polymer. The scattering from ligand/polymer complexes can then be described as $\bar{n}I_L + I_P/r$ where I_L and I_P are the scattering of 1 mg/mL solutions of free aFGF and free heparin, respectively. The concentration of free aFGF is given by $C_L - \bar{n}rC_P$ where C_L is the total amount of aFGF present in unliganded and bound forms.

Substituting these expressions into eq 1, an expression for $\bar{n}$ can then be obtained:

$$\bar{n} = \frac{1}{2}\left(1 - \frac{I_P}{rI_L} + \left(\left(1 - \frac{I_P}{rI_L}\right)^2 + 4\frac{C_L}{rC_P}\left(\frac{I - I_L}{I_L}\right)\right)^{1/2}\right) \qquad (2)$$

From the above equation, the stoichiometry of binding can be determined from known concentrations of aFGF and heparin and their corresponding intrinsic scattering intensities.

By analogy to the static light scattering model, the hydrodynamic radius (R) of aFGF/heparin mixtures can be expressed as a z-average of the R of both of the complexes and free aFGF in solution (Brown et al., 1975):

$$R = \frac{\sum C_i R_i^2}{\sum C_i R_i} \qquad (3)$$

After appropriate substitutions and solution for the radius of the polymer/ligand complex R_m, the following expression is obtained:

$$R_m = \frac{1}{2}\left(R + \left(R^2 + 4R_L(R - R_L)\left(\frac{C_L - \bar{n}rC_P}{\bar{n}rC_P}\right)\right)^{1/2}\right) \qquad (4)$$

where R_L and R are mean equivalent hydrodynamic radii of unbound ligand and the mixture of ligand, polymer, and polymer/ligand complexes, respectively. This permits the estimation of the apparent size of ligand/polymer complexes in the presence of unbound ligand.

Calculation of the Relative Dissociation Constants from Competition Experiments

The dissociation constants between ligand (aFGF) and heparin (K_d^H) and between the ligand (aFGF) and a competing compound (inositol hexasulfate) (K_d^I) are described by

$$K_d^H = \frac{c_L c_H}{c_{L,H}} \quad \text{and} \quad K_d^I = \frac{c_L c_I}{c_{L,I}} \qquad (5)$$

respectively. The symbols c_L, $c_{L,H}$, $c_{L,I}$, c_I, and c_H denote the molar concentrations of unbound aFGF, aFGF bound to heparin, aFGF bound to inositol hexasulfate, inositol hexasulfate, and heparin, respectively. It is assumed that there is no interaction between binding sites and that each aFGF molecule cannot bind to more than one heparin chain at any particular time. The above two equations can be combined to remove c_L, yielding after appropriate substitutions

$$\frac{K_d^H}{K_d^I} = \frac{(\bar{n}_{max} - \bar{n})c_H(\bar{n}_0 - \bar{n})}{\bar{n}(c_I - c_H(\bar{n}_0 - \bar{n}))} \qquad (6)$$

where the superscript H denotes heparin and I denotes inositol hexasulfate, $\bar{n}_{max}$ is the maximal number of aFGF molecules that can bind simultaneously to heparin, and $\bar{n}_0$ is the number of aFGF molecules bound in the absence of competing compounds.

Density and Partial Specific Volume Determinations

The density of the phosphate-buffered saline (PBS) and partial specific volume ($\bar{v}$) of polysaccharides were measured

by a Mettler-Paar DMA 60 density meter equipped with a DMA 602 density measuring cell. The $\bar{v}$ for aFGF was calculated from its amino acid composition (Cohn & Edsall, 1943) and found to be 0.73 mL/g. The $\bar{v}$ values for heparin and β-cyclodextrin were experimentally determined to be 0.510 and 0.453 mL/g, respectively. Values for the $\bar{v}$ of aFGF/polysaccharide complexes are calculated as weight averages: $\bar{v}_{complex} = \sum c_i \bar{v}_i / \sum c_i$.

Analytical Ultracentrifugation

Sedimentation equilibrium experiments were performed at 4 °C using a Beckman Optima XL-A analytical ultracentrifuge. Initial concentrations of 0.10, 0.25, and 0.50 mg/mL aFGF were loaded in the presence or absence of the indicated amount of polysaccharide. Centrifugation speeds ranging from 5000 to 30 000 rpm were employed. The data were collected by monitoring absorbance at 280 nm where only aFGF and its complexes absorb a significant amount of light with a negligible contribution from heparin itself.

The distribution of a sedimenting species is defined by the relation

$$\ln A_r = M(1 - v\rho)\omega^2 r^2 / 2RT \quad (7)$$

where A_r is the absorbance at 280 nm at radial position r (in centimeters), M is the molecular weight of the sedimenting species, ρ is the buffer solution density in grams/milliliter, ω is the angular velocity in radians/second, and R and T are the gas constant and temperature in Kelvin, respectively. Plotting ln A_r vs r^2, the slope will be proportional to M as defined by eq 7. Since a single-exponential fit is inadequate for associating systems in many cases, estimates of the weight-averaged M (M_w) can be obtained by linear regression of this plot in any region of the column.

Plasmon Resonance Analysis

All measurements were performed with a BIAcore system (Pharmacia Biosensor) and CM5 sensorchip as described by others (Karlsson et al., 1991; Jönsson et al., 1991; Chaiken et al., 1992).

(*a*) *Biotinylation of Heparin via Amino Groups* (*Lee & Conrad, 1984*). A 20 mg/mL solution of heparin in 0.3 M borate, pH 8.0, was incubated with a 3X molar excess of sulfo-NHS-biotin (Pierce) for 1 h at room temperature. Excess biotin was then removed on an NAP-5 column (Pharmacia). This chemically modified heparin is subsequently referred to as amino-biotinylated heparin.

(*b*) *Biotinylation of Heparin via Oxidized Cis-Diol Groups* (*O'Shannessy, 1990*). Oxidization of heparin (4.5 mg/mL) was performed at room temperature in 0.1 M sodium acetate, pH 5.5, containing 3.3 mM sodium metaperiodate. After a 1-h incubation, the oxidization was stopped by adding an excess of sodium sulfite. The heparin was further incubated with a 6-fold molar excess of biotin-x-hydrazide (Calbiochem) for 1 h. The excess biotin was then removed on an NAP-5 column. This form of heparin will be designated cis-diol biotinylated heparin.

(*c*) *Preparation of Sensor Surfaces.* Immobilization of streptavidin to sensorchip CM5 was performed by methodology described previously (Johnsson et al., 1991). During immobilization, the flow rate of the running buffer (PBS buffer, pH 7.2, containing 5 mM Na_2SO_4, 1 mM EDTA, and 0.05% Tween 20) was maintained at 5 μL/min. The surface was activated by injecting 8 μL of a mixture of EDC/NHS (0.2 M/0.05 M). Then, 30 μL of streptavidin (Sigma, 100 μg/mL in 10 mM sodium acetate, pH 4.5) was injected followed by 8 μL of ethanolamine hydrochloride, pH 8.5. The amount of streptavidin immobilized on the surface was 780 ± 30 RU (resonance units; see Results) for the two surfaces used. Onto each surface, 30 μL of biotinylated heparin was injected at a flow rate of 5 μL/min. Injection of amino-biotinylated and cis-diol biotinylated heparin produced 50 RU and 200 RU of immobilized material on the biosensor surface, respectively.

(*d*) *Affinity and Kinetics Determination of aFGF.* Stock aFGF solutions (1 mg/mL) were diluted in running buffer to various concentrations in the interval 10–500 nM and were injected onto the heparin surface. The injected volume of aFGF was 35 μL at a constant eluent flow of 5 μL/min. The heparinized biosensor surface was regenerated with 1.3 M NaCl in PBS (5 μL). Data points were collected continuously during the binding and dissociation processes and evaluated as described briefly in the text and in more detail elsewhere (Karlsson et al., 1991).

Structure of a Heparin Fragment Which Binds aFGF

Partial Digestion of Heparin. Porcine mucosal heparin, sodium salt, at 8 mg/mL was partially digested at 30 °C with 6 milliunits/mL of heparin lyase I in a solution of 0.2 M sodium chloride and 5 mM sodium phosphate at pH 7.0 (Lohse & Linhardt, 1992). Similarly, porcine intestinal mucosal and bovine lung heparin were treated with the same enzyme and when the reaction was 50%, 80%, or 100% complete, the heparin lyase I was thermally inactivated by heating at 100 °C for 1 min. The reaction was monitored by removing aliquots and measuring the product absorbance at 232 nm after 1:100 dilution into 0.03 N hydrochloric acid. After cooling, the aqueous solution was dialyzed in a 1000-M_r cutoff tubing against of distilled water. The pH of the dialyzed solution was adjusted to 6.0 and passed through a column of QAE-Sephadex to remove the enzyme, the pH was adjusted to 7.0, and the solution was redialyzed, frozen, and freeze-dried.

Preparation of Oligosaccharides. Oligosaccharides **1–4** were prepared by partial (at 80% reaction completion) digestion of bovine lung heparin with heparin lyase I and by preparative SAX–HPLC as previously reported (Rice & Linhardt, 1989; Linhardt et al., 1988, 1992). The structures of oligosaccharides **1–4** were also fully established (Al-Hakim & Linhardt, 1990), and their structures are shown in the Results section.

Digestion of Heparin Bound to Acidic Fibroblast Growth Factor. A solution of aFGF containing 1.33 mg/mL protein and 0.44 mg/mL heparin in 6 mM sodium phosphate and 120 mM sodium chloride, pH 7.25, was digested at 30 °C using 33 milliunits/mL of heparin lyase I, heparin lyase II, or a mixture 33 milliunits/mL heparin lyase I and 40 milliunits/mL heparin lyase II. After 15 h of incubation, the absorbance at 232 nm reached a maximum and the reaction was terminated by heating for 1 min at 100 °C. A control experiment used 0.44 mg/mL free heparin without any aFGF under identical conditions and the reaction was terminated after 15 h in the same manner. A second solution, containing 1.33 mg/mL of aFGF and 1.33 mg/mL of heparin in the same buffer was digested either using 36 milliunits/mL heparin lyase I or using 38 milliunits/mL heparin lyase I and 63 milliunits/mL heparin lyase II under identical reaction conditions. Aliquots containing 50 μg/40 μL product oligosaccharides were removed after 0, 0.5, 1, 2, 4, 6, 8, 18, and 24 h. Each sample was boiled for 1 min at 100 °C to thermally inactivate both the enzyme and aFGF, and both portions were analyzed using gradient PAGE.

Preparation of aFGF–Sepharose. CNBr-activated Sepharose (150 mg) was swelled in 10 mL of mM HCl, for 20 min and washed with 1 mM HCl, the coupling buffer (100 mM sodium bicarbonate, 500 mM sodium chloride, pH 8.3), and 6 mM sodium phosphate, 120 mM sodium chloride, pH 7.25 (equilibrating buffer). The gel suspension (1 mL) was transferred to a plastic vial containing aFGF/heparin complex (3:1), containing 1 mg of protein and heparin (0.33 mg) in 6 mM sodium phosphate, 120 mM sodium chloride, pH 7.25 coupling buffer and placed on a shaker for 2.5 h at room temperature. Residual CNBr groups on the Sepharose support were deactivated by shaking with 15 mL of 1 M ethanolamine in pH 8.0 buffer for 16 h at 4 °C and then extensively washed.

Affinity Fractionation of 50% Digested Porcine Mucosal Heparin. The aFGF–Sepharose (0.5 mL) was packed into a plastic column (0.5 × 2 cm), washed with elution buffer followed by equilibrating buffer, and loaded with a solution containing 1 mg of 50% digested porcine mucosal heparin in the equilibrating buffer and washed again with equilibrating buffer several times until the UV absorbance at 232 nm was negligible. Bound oligosaccharides were released using 2.5 mL of the elution buffer. The eluent containing high-affinity oligosaccharides was dialyzed in M_r 1000 cutoff tubing three times, frozen, and freeze-dried. Partially (50%) digested heparin (100 μg in 100 μL) in equilibrating buffer was loaded and the column was washed with 1.5 mL of equilibrating buffer. The washings containing low-affinity oligosaccharides were collected, dialyzed in the same manner, frozen, and freeze-dried.

Heparin that had been digested with heparin lyase I and II in the presence of soluble aFGF (3:1 as described above) was also fractionated on aFGF–Sepharose. Following enzymatic treatment, the aFGF was thermally inactivated and the insoluble protein was removed by centrifugation. The soluble heparin oligosaccharides were fractionated on aFGF–Sepharose and the high and low affinity fractions were collected and analyzed.

Digestion of Heparin Bound to aFGF–Sepharose Using Heparin Lyases. The aFGF–Sepharose containing approximately 1 mg of aFGF and 0.3 mg of bound porcine mucosal heparin was washed with 6 mM sodium phosphate buffer (pH 7.25) containing 120 mM of sodium chloride. A slurry was prepared using 1 mL of packed bed in 10 mL of the same buffer. A mixture of heparin lyase I (16 m-units/mL) and heparin lyase II (13 m-units/mL) was then added and the suspension was gently shaken at 30 °C for 3 h. The unbound oligosaccharides were collected and the bound oligosaccharides recovered by washing the beads with 6 mM sodium phosphate, 2 M sodium chloride, pH 7.25 (elution buffer). Both high and low affinity oligosaccharides were desalted and then concentrated by freeze-drying.

Gradient PAGE Analysis. Samples of free and protein-bound oligosaccharides as well as heparin were analyzed by applying each sample (10–50 μg in 20 μL of 50% sucrose solution) to a discontinuous PAGE gel (Rice et al., 1987) prepared by using a linear acrylamide and cross-linker gradient (12–22% total acrylamide).

RESULTS

Stoichiometry of aFGF/Heparin Complexes via Light Scattering Analysis. To determine the number of aFGF molecules that can bind to a single heparin polymer, the size of aFGF/heparin complexes were determined by static and dynamic light scattering. The changes in the ratio (I_+/I_-) of the static intensity of the scattered light of heparin/aFGF complexes (I_+) compared to the calculated intensity of

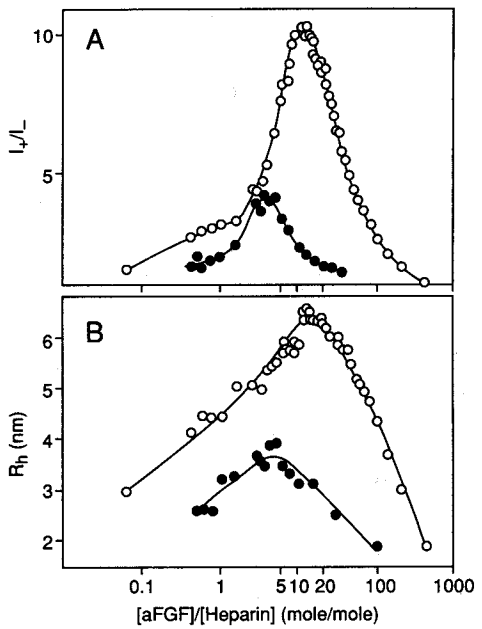

FIGURE 1: Size of aFGF/heparin complexes as a function of protein/polysaccharide molar ratio as measured by static and dynamic light scattering. (A) Scattered light intensity of the mixtures of aFGF and heparin (I_+) normalized to the sum of expected intensities from noninteracting aFGF and heparin (I_-). (B) Mean equivalent hydrodynamic radii of aFGF/heparin complexes at various ratios of protein to heparin. Symbols: (○) 16-kDa and (●) 4.8-kDa heparin. One milligram per milliliter aFGF solutions in PBS were titrated with concentrated stock solutions of heparin as described in the Materials and Methods section.

noninteracting protein and polysaccharide mixtures (I_-) are shown in Figure 1A. Initially, addition of heparin allows the formation of small amounts of aFGF/heparin complexes with resultant increases in the observed average scattering intensity. This increase in intensity will continue until all of the aFGF is bound. Further increases in the concentration of heparin, however, produce only partial occupancy of the now excess number of binding sites with a consequent decrease in the average complex size and the scattered light intensity. This decline observed upon the addition of heparin continues until there is on the average only one aFGF molecule bound per heparin chain. Only at this point does the increasing free heparin concentration begin to affect the observed total intensity and cause a further slow decrease. The titration maxima of the static light scattering responses (Figure 1A) occur at about 15:1 aFGF/heparin molar ratio for 16-kDa heparin and at about a 4:1 ratio for 4.8-kDa heparin. The results of a dynamic light scattering analysis (Figure 1B) follow a very similar pattern with maximal scattering occurring at the same aFGF/heparin ratios seen above.

From eq 2, it appears that under conditions of aFGF excess the maximum number of aFGF molecules that can bind to 16-kDa heparin is 14 (Figure 2A). This corresponds to approximately 4.4 monosaccharide units per aFGF molecule. It should be noted that the slope in Figure 2A for aFGF/heparin ratios of less than 10 has a value of unity which verifies the assumption of solution ideality. There is substantial deviation from ideal behavior, however, at aFGF/16-kDa heparin ratios in the range of 10–20 (Figure 2A). One possible explanation is that the aFGF sites on heparin do not bind the protein with equal affinity. Visual inspection of the data is most consistent with approximately 10 high-affinity sites and 4 low-affinity ones. Alternatively, the absence of distinct, discrete binding sites for aFGF on heparin is also consistent with these observations. Instead, aFGF molecules might bind

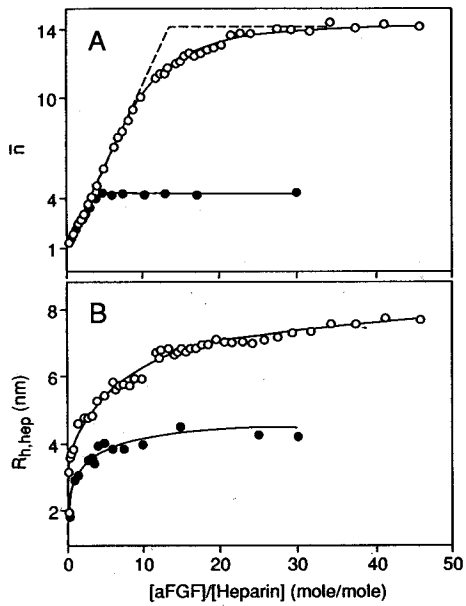

FIGURE 2: Modeling of the stoichiometry of aFGF/heparin complexes as the ratio of the two components is varied during light scattering experiments (see text). (A) The average number of aFGF molecules bound to one heparin chain ($\bar{n}$) as determined from eq 2. (B) The mean equivalent hydrodynamic diameter of aFGF/heparin complexes as calculated from eq 4. Symbols: (○) 16-kDa and (●) 4.8-kDa heparin.

at random locations along the heparin chain. This would decrease the efficiency of aFGF binding at higher levels of the protein since the gaps between bound aFGF molecules would become less than the minimum necessary size and thus be filled with greater difficulty.

The values of the mean equivalent hydrodynamic radii of aFGF/heparin aggregates found from eq 4 follow the pattern observed in the static light scattering measurements (Figure 2B). Under conditions of aFGF excess, the mean hydrodynamic radius of the complex is about 7 nm. The hydrodynamic radius slightly enlarges as the amount of free aFGF is further increased. This may be due to the weak binding of a few additional aFGF molecules which are only detectable in the presence of a large excess of protein. A protein sphere of 7-nm radius with a typical density of 1.33 g/cm^3 would possess a corresponding molecular weight of 1 100 000 for 16 kDa and 220 000 for 4.8-kDa heparin, respectively. Since the actual molecular weight of aFGF saturated heparin complexes is about 250 000 and 70 000 (assuming 15 and 4.4 aFGF molecules per heparin chain, respectively), this calculation suggests that the overall shape of aFGF/heparin complexes is significantly elongated.

To further explore the quantitative nature of the interaction of aFGF with heparin, mixtures of various ratios were titrated with the low molecular weight polyanion inositol hexasulfate (IHS) which also binds to aFGF at the heparin binding site (Volkin et al., 1992, 1993). Comparison of the relative slopes of plots of $\bar{n}$ vs [IHS]/[aFGF] at various aFGF/heparin ratios suggests that at low occupancies of heparin binding sites [aFGF/heparin = 6.5:1] no aFGF molecules are dissociated in the presence of up to a 10-fold excess of IHS (not illustrated). Saturated (20:1) or nearly saturated (13:1) heparin molecules, however, do begin to lose some of their bound aFGF molecules at low concentrations of the competing polyanion. This implies that a fraction of available heparin binding sites have weaker affinity. Using eq 6, the ratio of the K_d of aFGF dissociation from heparin to that from IHS is found to be 0.0058 ± 0.0012 for the strongest aFGF binding sites.

Estimation of aFGF/Heparin Stoichiometry by Analytical Ultracentrifugation. As a second approach to determine the size (and stoichiometry) of the aFGF/heparin complexes, their molecular weights were estimated by sedimentation equilibrium experiments. Since polyelectrolytes such as heparin exhibit nonideal behavior due to their high charge content (Braswell, 1968), application of a single equilibrium exponential model without appropriate correction may seem questionable. Nevertheless, when experimental analytical ultracentrifugation data for aFGF in the presence of a 3-fold excess of heparin were analyzed with the inclusion of nonideality and association terms, no improvement in the fit of the data compared to the single species model was found (E. Braswell, personal communication). Thus, assuming ideal single species behavior under conditions of equimolar or excess heparin seems to be a reasonable approximation in this system at least for comparative purposes. The relatively high ionic strength of the PBS employed may produce sufficient charge shielding to substantially reduce contributions from nonideal behavior. Application of this simple model to the ultracentrifugation data of aFGF with equimolar and a 3-fold excess of heparin yields a molecular mass of 30–35 kDa for the heparin/aFGF complex in both cases (not illustrated).

Equilibrium sedimentation experiments for ratios of heparin/aFGF of less than unity indicate that the system is no longer homogeneous. A distribution of molecular weights of the complex is expected as multiple aFGF molecules attach to single heparin molecules. Since the amount of bound aFGF is also dependent on the size of the heparin molecule, the known heterogeneity in heparin size will add additional variability as each molecule becomes saturated with the growth factor. For a 1:3 ratio of heparin to aFGF, the molecular masses obtained near the meniscus and the bottom of the column are 40 and 80 kDa, respectively. A 10-fold excess of aFGF produces an even wider distribution of molecular masses ranging from 50 to 160 kDa (not illustrated). This corresponds to aFGF/heparin ratios of approximately 2:1 and 9:1, respectively.

Affinity of Heparin–aFGF Interactions Examined by Surface Plasmon Resonance. To further quantitatively characterize the affinity of aFGF to heparin, the equilibrium and time dependence of the binding process were examined by surface plasmon resonance biosensor technology. This technique monitors the real-time binding of protein molecules to an immobilized ligand by passing a protein solution over on a dextran derivatized sensor chip surface (Fägerstam et al., 1990; Karlsson et al., 1991; Jönnson et al., 1991; Chaiken et al., 1992). This detection is achieved by measuring refractive index changes near a thin gold surface deposited on glass (Kretschmann & Raether, 1968; Liedberg et al., 1983; Cullen et al., 1987, 1988). When the refractive index in the vicinity of the gold surface is altered, the angle at which plasmon resonance occurs is correspondingly modified. These changes, measured in resonance units (RU), directly correlate with the amount of protein interacting with the surface (Stenberg et al., 1991). One resonance unit is approximately equivalent to 1 pg bound/mm^2.

Biotinylated heparin was immobilized to the biosensor through specific, noncovalent interactions with streptavidin covalently linked to the carboxylated dextran matrix on the sensor surface (Johnsson et al., 1991). A solution of aFGF is injected into a flow cell and passed over the heparinized surface of the biosensor. Several phases in the binding of aFGF to the heparinized surface can be identified in sensorgrams (a plot of the refractive index change in resonance

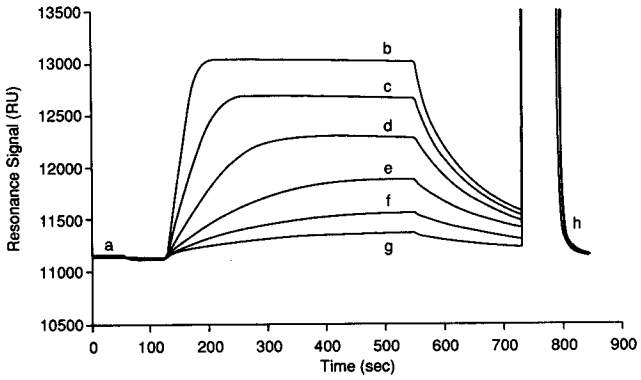

FIGURE 3: Surface plasmon resonance sensorgram of the association and dissociation of aFGF to a heparinized biosensor surface. Varying amounts of aFGF were injected over a heparinized biosensor (cis-diol biotinylated heparin bound to a streptavidin-biosensor surface), and the amount of protein associating/dissociating from the surface over time was measured in resonance units (RU) as described in the text. (a) PBS running buffer containing 6 mM phosphate, 120 mM NaCl, 1 mM EDTA, 5 mM Na_2SO_4, and 0.05% Tween 20 at pH 7.2; (b) 500 nM; (c) 250 nM; (d) 125 nM; (e) 62 nM; (f) 31 nM; (g) 16 nM aFGF in PBS running buffer; (h) regeneration of heparinized biosensor surface with PBS running buffer containing 1.3 M NaCl.

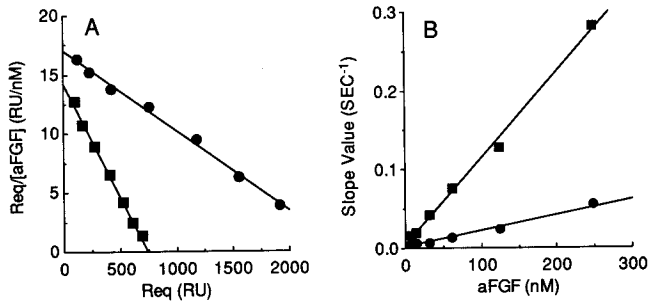

FIGURE 4: Steady-state and kinetic analysis of the interaction of aFGF with two different heparinized biosensor surfaces as measured by surface plasmon resonance. (A) Scatchard plot of the steady-state plasmon resonance response (Req; in resonance units, see Figure 3 and text) as a function of Req divided by the aFGF concentration injected over the heparinized biosensor surface. (B) Kinetic analysis of the slope (from dR/dt vs RU response plot; see text) as a function of various aFGF concentrations injected over the heparinized biosensor surface. Symbols: (■) Amino-biotinylated heparin and (●) cis-diol-biotinylated heparin. Preparation of both the biotinylated heparin and biosensor surfaces are described in the Materials and Methods section.

units (RU) versus time). Figure 3 is an overlay of several sensorgrams which result when varying amounts of aFGF were passed over a heparinized biosensor surface. The baseline levels (the period 0–150 s) reflect the effect of running buffer alone. As the aFGF solution passes over the biosensor chip, the protein binds to the surface in two phases (~150–400 s): mass transport limited and reaction rate (k_{on}) limited. A steady-state level of aFGF on the surface is then reached (400–550 s), representing the equilibrium binding of aFGF to immobilized heparin. Finally, as the running buffer without aFGF is reintroduced (>550 s), a time-dependent dissociation of aFGF from the biosensor surface is observed.

The equilibrium RU values from the sensorgrams of aFGF binding to biotinylated heparin surfaces (Figure 3) were utilized to construct Scatchard plots, R_{eq}/C vs R_{eq}, where R_{eq} is the equilibrium response in RU and C is the free aFGF concentration (the concentration of aFGF injected into the flow cell). As shown in Figure 4A, Scatchard analysis of the binding of varying amounts of aFGF to the biotinylated heparin surface yields K_d values of 50 and 140 nM for the interaction with heparin biotinylated via amino or oxidatively generated aldehyde groups, respectively (see Materials and Methods).

A kinetic analysis of the sensorgrams from the interaction of aFGF with immobilized heparin was based on the following expression (Karlsson et al., 1991):

$$\frac{dR}{dt} = k_{on}CR_{max} - (k_{on}C + k_{off})R \qquad (8)$$

where R is the plasmon-resonance response (RU) due to aFGF interaction with the heparinized surface, k_{on} and k_{off} are the association (M^{-1} s^{-1}) and dissociation (s^{-1}) rate constants, respectively, C is the concentration of injected aFGF, and R_{max} is the RU response at saturation of heparin binding sites. It can be shown that k_{on} may be determined from the association phase of the sensorgram, i.e., the slope of a plot of aFGF concentration versus the slopes of dR/dt dependence on RU response (Karlsson et al., 1991). Values for k_{off} can be calculated during the dissociation phase of the sensogram since as $C \rightarrow$ zero, the decay rate ($-dR/dt$) gives k_{off} (see eq 8).

An analysis of the association rate constant for the interaction of aFGF with immobilized heparins is shown in Figure 4B. By first plotting the binding rate (dR/dt) vs the RU response, the mass transport vs reaction limited phases of association can be separately determined using standard procedures (Karlsson et al., 1991). The initial mass transport limited phase was characterized by a constant binding rate with increasing response. Near equilibrium, the intrinsic reaction rate becomes lower than the rate of mass transport, causing the binding rate to decrease linearly with response (data not shown). A best-fit straight line to the reaction rate limited part of the plot gives slope values equal to $Ck_{on} + k_{off}$ which are plotted against aFGF concentration in Figure 4B. The association rate constants (k_{on}) for the cis-diol and amino-biotinylated heparin are found to have values of 1.9×10^5 M^{-1} s^{-1} and 1.1×10^6 M^{-1} s^{-1}, respectively. The association rate constant for the amino-biotinylated heparin is approximately five times higher than the cis-diol-biotinylated heparin, further supporting the importance of the nature of the chemical modification of heparin on these measurements. Although the direct determination of the dissociation rate constant during the dissociation phase was attempted (Karlsson et al., 1991), the ability of aFGF to rebind the heparinized surface after the initial dissociation complicated this analysis. The dissociation rate constant was determined directly from $K_d = k_{off}/k_{on}$, giving values of 0.06 s^{-1} and 0.03 s^{-1} for amino- and cis-diol-biotinylated heparin, respectively.

An estimate of the number of aFGF molecules that bind to heparin can be performed employing the following equation (BIAcore System Manual, Pharmacia Biosensor, copyright 1991):

$$S = \left(\frac{R_{max(aFGF)}}{R_{(immobheparin)}}\right)\left(\frac{MW_{immobheparin}}{MW_{aFGF}}\right) \qquad (9)$$

where $R_{max(aFGF)}$ is the maximum aFGF binding capacity of the heparinized surface in RU, $R_{(immobheparin)}$ is the amount of ligand on the biosensor surface in RU, and MW is molecular weight of heparin and aFGF. $R_{max(aFGF)}$ can be estimated from extrapolation of the Scatchard plot (Figure 4A) to be approximately 750 and 2500 RU for amino- and cis-diol-biotinylated heparin, respectively. The amount of heparin on the surface is estimated to be 50 and 200 RU, respectively (see Materials and Methods). Since RU is proportional to the refractive index increment (Stenberg et al., 1991), a correction factor for heparin RU values is based on the ratio of values for the refractive index increment of aFGF and heparin (measured as 0.197 mL/g for protein and 0.124 mL/g

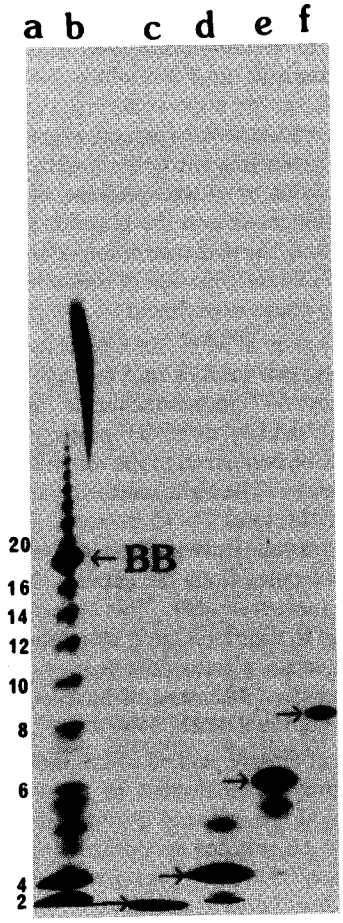

FIGURE 5: Gradient PAGE analysis of heparin and heparin oligosaccharide standards. Conditions are described in the Materials and Methods section. Lane a: Ladder of standard heparin oligosaccharides labeled by degree of polymerization prepared by the partial (50%) depolymerization of bovine lung heparin using heparin lyase I. Lane b: Porcine mucosal heparin. Lane c: Disaccharide standard **1**. Lane d: Tetrasaccharide standard **2**. Lane e: Hexasaccharide standard **3**. Lane f: Octasaccharide standard **4**. The chemical structures of these heparin lyase derived heparin oligosaccharides are shown in the text. The bands above the bromophenol blue tracking dye (BB) correspond to high molecular weight oligosaccharides of dp > 20 (or $n > 9$).

for heparin) and is estimated to be 1.58. This calculation results in 8–10 aFGF molecules bound per heparin molecule.

Chemical Nature of the aFGF Binding Site of Heparin. To examine the size requirements for a heparin oligosaccharide binding to aFGF, the heparin lyase catalyzed digestion of heparin bound to aFGF in solution was employed followed by gradient PAGE analysis of the resulting oligosaccharide products. Figure 5 shows that heparin alone runs well into the resolving gel (Figure 5, lane b) and that oligosaccharides from partially digested bovine lung heparin form a ladder of bands (lane a). Several of these bands can be directly assigned using defined oligosaccharide standards **1**–**4** (Figure 5, lanes c–f):

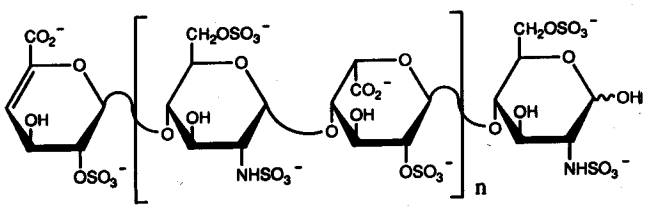

In disaccharide **1**, $n = 0$; in tetrasaccharide **2**, $n = 1$; in hexasaccharide **3**, $n = 2$; and in octasaccharide **4**, $n = 3$.

In initial experiments, aFGF solutions containing 1/3 heparin by weight were digested using 10 milliunits/mL of heparin lyase I for 15 h at 30 °C. To analyze heparin or oligosaccharide bound to aFGF by gradient PAGE, these complexes were first dissociated by heating for 1 min at 100 °C prior to electrophoretic analysis. PAGE analysis of the product indicated only partial digestion of the heparin. A wide range of reaction conditions gave comparable protection of the heparin's oligosaccharide binding sites. The only oligosaccharides found to be enriched were oligosaccharides of octasaccharide size and larger (particularly dp 20–28).

These results suggested that heparin lyase I might be unable to trim some unbound monosaccharide units from around bound aFGF molecules. To test this hypothesis, we employed heparin lyase II. While heparin lyase I is a very specific endolytic enzyme, heparin lyase II is considerably less specific (Linhardt et al., 1982, 1990). When heparin lyase II was used to treat aFGF/heparin complexes, the results obtained were remarkably similar to those seen for heparin lyase I. Once again, the aFGF protected heparin sequences corresponding to oligosaccharides of size larger than octasaccharides. Heparin lyases can act synergistically to nearly completely digest heparin (Ampofo & Linhardt, 1992). By treating the aFGF/heparin complex with a mixture of these two enzymes, the higher oligosaccharides nearly disappeared giving rise to an intense band corresponding in size to a tetrasaccharide (Figure 6, lane e). This protected oligosaccharide comigrated on gradient PAGE with tetrasaccharide **2**.

A second approach to examine the size requirements of oligosaccharide binding to aFGF made use of aFGF affinity chromatography to isolate oligosaccharides with a high affinity for aFGF. Porcine mucosal heparin (157 units/mg) was partially digested (50%) using heparin lyase I to obtain a mixture of oligosaccharides. This oligosaccharide mixture was affinity fractionated on an aFGF–Sepharose column. Oligosaccharides not retained by the column were assigned low-affinity status. Oligosaccharides bound on the column and released by 2 M sodium chloride were designated high-affinity oligosaccharides. The results from this experiment are shown in Figure 6, lanes a–c. These results again demonstrate that not only do heparin derived hexa- and higher oligosaccharides strongly bind to aFGF, but the same intense band, corresponding to a protected oligosaccharide comigrating with tetrasaccharide **2**, is enriched in the high-affinity and depleted in the low-affinity fractions.

Footprinting and aFGF affinity chromatography techniques were used in combination. Soluble aFGF bound to heparin was digested with a mixture of heparin lyase I and II. After aFGF protected digestion, these oligosaccharides were affinity fractionated. The high-affinity oligosaccharides are found enriched in high molecular weight components (dp 10, 12, 14) while the low-affinity oligosaccharides are reduced in the same species. Again, a protected oligosaccharide comigrating with tetrasaccharide **2** is enriched in the high-affinity mixture and depleted in the low-affinity mixture.

The purified tetrasaccharide standard **2** was examined for its ability to associate and dissociate from immobilized aFGF. The tetrasaccharide was applied to a column containing covalently attached aFGF, and elution was attempted with concomitant monitoring of the absorbance of the tetrasaccharide (ϵ_M = 5200 at 232 nm) (Rice & Linhardt, 1989; Linhardt et al., 1988). It was found that all of the tetrasaccharide bound to the aFGF–Sepharose column and could be released by heparin or 2 M sodium chloride. The tetrasaccharide failed to bind to aFGF–Sepharose after the immo-

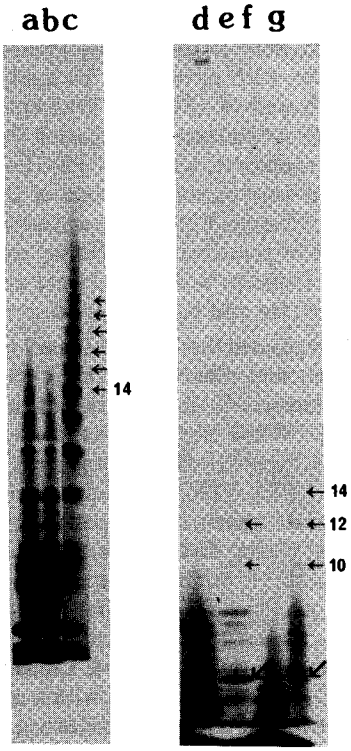

FIGURE 6: Gradient PAGE analysis of 50% digested heparin and soluble aFGF–heparin treated with a mixture of heparin lyase I and II. Lane a: Porcine heparin which was partially (50%) digested using heparin lyase I. Lane b: 50% digested heparin (with heparin lyase I) having low affinity for aFGF–Sepharose. Lane c: 50% digested heparin having high affinity for aFGF–Sepharose. Lane d: heparin treated with heparin lyase I and II. Lane e: heparin bound to soluble aFGF (3:1) treated with heparin lyases I and II. Lanes f and g: heparin bound to soluble aFGF treated with heparin lyases I and II in which the aFGF is thermally inactivated and removed by centrifugation and the heparin oligosaccharides are then passed through an aFGF–Sepharose column. Lane f: low-affinity fraction. Lane g: high-affinity fraction. The horizontal arrows indicate the bands corresponding to high molecular weight oligosaccharides interacting with aFGF while the oblique arrows near the bottom of the gel indicate the enriched tetrasaccharide in lanes e and g.

bilized aFGF had been thermally inactivated by heating (100 °C). In addition, when purified aFGF was noncovalently bound to a heparin–Sepharose column, a PBS solution containing the tetrasaccharide was able to displace the protein from the heparinized resin.

DISCUSSION

A variety of indirect evidence suggests that multiple species of acidic and basic FGF can bind to heparin polymers. For example, Sommer and Rifkin (1989) reported complete protection of bFGF against proteolytic digestion at a growth factor to heparin ratio of 10–13. Furthermore, insoluble bFGF/heparin complexes were found to form at protein/polysaccharide ratios of 8–10 (w/w) with 16-kDa heparin suggested to bind up to a 10-fold excess of bFGF. Similarly, we previously found that the midpoint of heparin's ability to protect aFGF against both thermal unfolding and heat-induced aggregation occurs when the growth factor is present at a 10-fold molar excess over heparin (Copeland et al., 1991; Volkin et al., 1992, 1993). In contrast, Lee and Lander (1991) concluded from electrophoretic shift experiments that the interaction of bFGF with heparin is monovalent.

Both static and dynamic light scattering measurements indicate that approximately 14–15 molecules of aFGF are capable of binding to a single molecule of 16-kDa heparin. This approximate stoichiometry was confirmed by both sedimentation analysis and a surface plasmon resonance technique. The latter two approaches give slightly lower values (aFGF/heparin = 9 and 8–10, respectively) which may reflect the difficulty in saturating the heparin with aFGF due to the lower concentrations employed and the derivatization (biotinylation) of the heparin in the plasmon resonance experiments. In addition, the presence of low-affinity binding sites may result in an underestimation of the total number of sites as determined in these experiments.

If 10–15 molecules of aFGF can bind to a single 16-kDa heparin molecule, this implies that one aFGF molecule can be present every 5–7 monosaccharide units. This is a surprisingly high density of aFGF molecules on a heparin chain and should be compared to the tetrasaccharide binding site discussed below. The light scattering studies imply that several (3–5) of the total 14–15 potential binding sites are rather weak, but a relatively uniform distribution of closely spaced aFGF molecules along the heparin chain is consistent with all of these measurements. This high density of binding can be contrasted to the much lower stoichiometry seen in the interaction of human plasma low-density lipoprotein with heparin (Gigli et al., 1992) and of human factor XII with dextran sulfate (Samuel et al., 1992).

The presence of closely packed aFGF molecules along the heparin chain may be analogous to the dimerization and trimerization of bFGF induced by heparin fragments containing 6, 8, and 16 sulfated monosaccharide units seen by others (Ornitz et al., 1992). This latter work also found that an octasaccharide of heparin was the smallest unit capable of supporting the binding of bFGF to its cell surface receptor and consequent mitogenic activity. Our finding of octasaccharides as the primary product in the aFGF/heparin protection experiments when a single heparin lyase is employed may also reflect the stability of aFGF dimers along the oligosaccharide chain. On the basis of these observations, the authors speculate that polyanion-mediated cross-linking of bFGF may lead to dimerization of its cell surface receptor (Ornitz et al., 1992). This situation may be analogous to that of many tyrosine kinase growth factor receptors in which it is thought that receptor dimerization is an early event in activation of intracellular responses (Ullrich & Schlessinger, 1990). Our work with heparin and aFGF would suggest that microaggregation above that of a dimer might occur as a result of the high stoichiometry of a single heparin (and presumably on highly sulfated regions of heparan sulfate) polymer. Preliminary light scattering experiments indicate that one aFGF molecule binds approximately 5–6 monosaccharide units of heparan sulfate, but this material appears to have a higher fraction of low-affinity sites compared to heparin (not illustrated).

The plasmon resonance studies also permit an estimate of the dissociation constant of aFGF for heparin, which is found to be on the order of 50–140 nM and is in excellent agreement with that obtained from affinity electrophoresis experiments (91 nM; Lee & Lander, 1991). The chemical modifications used in these experiments alter different functional groups of heparin to varying extents (Helbert & Marini, 1963; Chung & Ellerton, 1976), so it is not surprising that a range of K_d, k_{on}, and k_{off} values was observed on the two surfaces.

This study also finds that the tetrasaccharide **2** binds to aFGF. Footprinting experiments demonstrate that soluble aFGF (Figure 6d–g) protects an oligosaccharide that comigrates with tetrasaccharide **2** along with larger fully sulfated

oligosaccharides (see structures). Also, on treatment of immobilized aFGF/heparin complex with a mixture of heparin lyase I and II, this protected oligosaccharide comigrating with tetrasaccharide **2** is recovered still bound to aFGF (not shown). Both of these experiments argue that this particular oligosaccharide is preferentially protected by aFGF. This preferential binding might be explained by the high charge of this oligosaccharide. We have previously demonstrated that increasing sulfation or phosphorylation of small polyanions enhances their ability to stabilize aFGF (Volkin et al., 1992, 1993). The binding of tetrasaccharide **2** (which comigrates with the protected oligosaccharide) to aFGF can be disrupted by the use of buffer containing high salt consistent with an ionic interaction. A tetrasaccharide prepared by controlled nitrous acid depolymerization (Barzu et al., 1989) contained one less sulfate group than tetrasaccharide **2** and also had a ring-contracted anhydromannose residue at its reducing terminus. These structural differences may be responsible for the failure of this previous study to observe an interaction between a heparin-derived tetrasaccharide and aFGF. A synthetic pentasaccharide having high affinity for antithrombin III as well as potentiating aFGF mitogenic activity (Uhlrich et al., 1986) has 7 sulfate groups as compared to the 6 sulfates found in tetrasaccharide **2**.

Thus, these results suggest the resistance of a single oligosaccharide to enzymatic digestion. This protected oligosaccharide comigrates with **2**, a hexasulfated tetrasaccharide of sufficient size and charge to interact with aFGF. This interaction is also sufficiently stable to at least partially protect other highly sulfated oligosaccharides (including oligosaccharides comigrating with hexasaccharide **3** and octasaccharide **4**, a dimer of tetrasaccharide **2**) against digestion by single or mixtures of heparin lyases. The selectivity of this binding is suggested by the failure of this experiment to enrich multiple tetrasaccharides. It thus appears that aFGF contains what is essentially a well-defined tetrasaccharide-sized binding site, although its specificity may be rather low other than the requirement for a high negative charge density. Tetrasaccharide **2**, which comigrates with aFGF-protected oligosaccharide, has been previously shown to be the minimum size heparin fragment necessary to stabilize aFGF to thermal unfolding (Volkin et al., 1992, 1993). This tetrameric sequence is known to be dispersed widely in heparin and related proteoglycans and may appear with sufficient regularity to account for the frequent binding sites present in heparin polymers. Differences in the pattern and degree of sulfation between heparin and heparan sulfate may be important in this regard. In contrast to heparin, regions of extensive sulfation appear to be clustered in cell surface heparan sulfates (Gallagher et al., 1992). These regions might thus be expected to be correspondingly enriched in aFGF molecules.

ACKNOWLEDGMENT

We thank Dr. Emory Braswell for his assistance in analyzing the sedimentation data and Laurie Rittle for her preparation of the manuscript.

REFERENCES

Al-Hakim, A., & Linhardt, R. J. (1990) *Electrophoresis 11*, 23–28.

Ampofo, S. A., & Linhardt, R. J. (1992) *Anal. Biochem. 199*, 249–255.

Barzu, T., Lormeau, J. C., Petitou, M., Michelson, S., & Choay, J. (1989) *J. Cell. Physiol. 140*, 538–548.

Braswell, E. (1968) *Biochim. Biophys. Acta 158*, 103–116.

Brown, J. C., Pusy, P. N., & Dietz, R. (1975) *J. Chem. Phys. 62*, 1136–1144.

Burgess, W. H., & Maciag, T. (1989) *Annu. Rev. Biochem. 58*, 575–606.

Chaiken, I., Rosé, S., & Karlsson, R. (1992) *Anal. Biochem. 201*, 197–210.

Chung, M. C. M., & Ellerton, N. F. (1976) *Biopolymers 15*, 1409–1423.

Cohn, E. J., & Edsall, J. T. (1943) *Proteins, Amino Acids and Peptides as Ions and Dipolar Ions*, pp 374–377, Hafner, New York.

Copeland, R. A., Ji, H., Halfpenny, A. J., Williams, R. W., Thompson, K. C., Herber, W. K., Thomas, K. A., Bruner, M. W., Ryan, J. A., Marquis-Omer, D., Sanyal, G., Sitrin, R. D., Yamazaki, S., & Middaugh, C. R. (1991) *Arch. Biochem. Biophys. 289*, 53–61.

Cullen, D. C., Brown, R. G. W., & Lowe, C. R. (1987/1988) *Biosensors 3*, 211–225.

Dabora, J. M., Sanyal, G., & Middaugh, C. R. (1991) *J. Biol. Chem. 2662*, 23637–23640.

Eriksson, A. E., Cousens, L. S., Weaver, L. H., & Matthews, B. W. (1991) *Proc. Natl. Acad. Sci. U.S.A. 88*, 3441–3445.

Fägerstam, L. G., Frostell, A, Karlsson, R., Kullman, M., Larson, A., Malmqvist, M., & Butt, H. (1990) *J. Mol. Recognit. 3*, 208–214.

Gallagher, J. T., Turnbull, J. E., & Lyon, M. (1992) *Int. J. Biochem. 24*, 553–560.

Gigli, M., Consonni, A., Ghiselli, G., Rizzo, V., Naggi, A., & Torri, G. (1992) *Biochemistry 31*, 5996–6003.

Helbert, J. R., & Marini, M. A. (1963) *Biochemistry 2*, 1101–1106.

Jackson, R. L., Busch, S. J., & Cardin, A. D. (1991) *Physiological Rev. 71*, 481–539.

Johnsson, B., Löfås, S., & Lindquist, G. (1991) *Anal. Biochem. 198*, 268–277.

Jönsson, U., Fägerstam, L., Ivarsson, B., & Johnsson, B. (1991) *BioTechniques 11*, 620–627.

Karlsson, R., Michaelsson, A., & Mattsson, L. (1991) *J. Immunol. Methods 145*, 299–310.

Koppel, D. E. (1972) *J. Chem. Phys. 57*, 4814–4820.

Kretschmann, E., & Raether, H. (1968) *Z. Naturforsch. A 23*, 2135–2136.

Lee, W. T., & Conrad, D. H. (1984) *J. Exp. Med. 159*, 1790–1795.

Lee, M. K., & Lander, A. D. (1991) *Proc. Natl. Acad. Sci. U.S.A. 88*, 2768–2772.

Liedberg, B., Nylander, C., & Lundström (1983) *Sens. Actuators 4*, 299–304.

Linemeyer, D. L., Kelly, L. J., Menke, J. G., Gimenez-Gallego, G., DeSalvo, J., & Thomas, K. A. (1987) *Biotechnology 5*, 960–965.

Linhardt, R. J., Fitzgerald, G. L., Cooney, C. L., & Langer, R. (1982) *Biochim. Biophys. Acta 702*, 197–203.

Linhardt, R. J., Rice, K. G., Kim, Y. S., Lohse, D. L., Wang, H. M., & Loganathan, D. (1988) *Biochem. J. 254*, 781–787.

Linhardt, R. J., Turnbull, J. E., Wang, H. M., Loganathan, D., & Gallagher, J. T. (1990) *Biochemistry 29*, 2611–2617.

Linhardt, R. J., Wang, H. M., Loganathan, D., & Bae, J. H. (1992) *J. Biol. Chem. 267*, 2380–2387.

Lohse, D. L., & Linhardt, R. J. (1992) *J. Biol. Chem. 267*, 24347–24355.

Middaugh, C. R., Mach, H., Burke, C. J., Volkin, D. B., Dabora, J. M., Tsai, P. K., Bruner, M. B., Ryan, J. A., & Marfia, K. E. (1992) *Biochemistry 31*, 9016–9024.

Moscatelli, D. (1987) *J. Cell. Physiol. 131*, 123–130.

Ornitz, D. M., Yayon, A., Flanagan, J. G., Svahn, C. M., Levi, E., & Leder, P. (1992) *Mol. Cell. Biol. 12*, 240–247.

O'Shannessy, D. J. (1990) *Methods Enzymol. 184*, 162–166.

Petitou, M., Lormeau, J. C., & Choay, J. (1991) *Nature 350* (Suppl.), 30–33.

Rice, K. G., & Linhardt, R. J. (1989) *Carbohydr. Res. 190*, 219–233.
Rice, K. G., Rottink, M. D., & Linhardt, R. J. (1987) *Biochem. J. 244*, 515–522.
Samuel, M., Pixley, R. A., Villanueva, M. A., Colman, R. W., & Villanueva, G. B. (1992) *J. Biol. Chem. 267*, 19691–19697.
Sommer, A., & Rifkin, D. B. (1989) *J. Cell. Physiol. 138*, 215–220.
Stenberg, E., Persson, B., Roos, H., & Urbaniczky, C. (1991) *J. Colloid Interface Sci. 143*, 513–526.
Sudhalter, J., Folkman, J., Svahn, C. M., Bergendal, K., & D'Amore, P. A. (1989) *J. Biol. Chem. 264*, 6892–6897.
Tanford, C. (1961) *Physical Chemistry of Macromolecules*, pp 275–316, John Wiley & Sons, New York.
Thomas, K. A., Rios-Candelore, M., & Fitzpatrick, K. (1984) *Proc. Natl. Acad. Sci. U.S.A. 81*, 357–361.
Uhlrich, S., Lagente, O., Choay, J., Courtois, Y., & Lenfant, M. (1986) *Biochem. Biophys. Res. Commun. 139*, 728–732.
Vlodavsky, I., Fuks, Z., Ishai-Michaeli, R., Bashkin, P., Levi, E., Korner, G., Bar-Shavit, R., & Klagsbrun, M. (1991) *J. Cell. Biochem. 45*, 167–176.
Volkin, D. B., Tsai, P. K., Dabora, J. M., & Middaugh, C. R. (1992) in *Harnessing Biotechnology for the 21st Century* (Ladisch, M. R., & Bose, A., Eds.) pp 298–302, American Chemical Society, Washington, D.C.
Volkin, D. B., Tsai, P. K., Dabora, J. M., Gress, J. O., Burke, C. J., Linhardt, R. J., & Middaugh, C. R. (1993) *Arch. Biochem. Biophys. 300*, 30–41.
Walicke, P. A., Feige, J. J., & Baird, A. (1989) *J. Biol. Chem. 264*, 4120–4126.
Zhang, J., Cousens, L. S., Barr, P. J., & Sprang, S. R. (1991) *Proc. Natl. Acad. Sci. U.S.A. 88*, 3446–3450.
Zhu, X., Komiya, H., Chirino, A., Faham, S., Fox, G. M., Arakawa, T., Hsu, B. T., & Rees, D. C. (1991) *Science 251*, 90–93.